

Seismic response control of buildings with force saturation constraints

Filippo Ubertini* and A. Luigi Materazzi

Department of Civil and Environmental Engineering, University of Perugia, Perugia 06125, Italy

(Received August 1, 2012, Revised October 15, 2012, Accepted January 12, 2013)

Abstract. We present an approach, based on the state dependent Riccati equation, for designing non-collocated seismic response control strategies for buildings accounting for physical constraints, with particular attention to force saturation. We consider both cases of active control using general actuators and semi-active control using magnetorheological dampers. The formulation includes multi control devices, acceleration feedback and time delay compensation. In the active case, the proposed approach is a generalization of the classic linear quadratic regulator, while, in the semi-active case, it represents a novel generalization of the well-established modified clipped optimal approach. As discussed in the paper, the main advantage of the proposed approach with respect to existing strategies is that it allows to naturally handle a broad class of non-linearities as well as different types of control constraints, not limited to force saturation but also including, for instance, displacement limitations. Numerical results on a typical building benchmark problem demonstrate that these additional features are achieved with essentially the same control effectiveness of existing saturation control strategies.

Keywords: structural control; seismic structural protection; active bracing systems; magnetorheological dampers; state dependent Riccati equation

1. Introduction

The seismic protection of civil engineering structures through response control strategies is a promising research field that, however, still presents several open issues. In fact, differently from strategies designed to satisfy limit states criteria under wind loads (Yan *et al.* 1999, Varadarajan and Nagarajaiah 2004) whose return periods can be relatively short (Gusella and Materazzi 1998, Hong *et al.* 2011), the activation of the system in the unpredictable moment of the earthquake is still a rather problematic issue. Another major concern is represented by the physical constraints that limit the performances and the reliability of control devices. Such limitations, like force saturation (Forrai *et al.* 2003, Cao *et al.* 2004, Ying *et al.* 1997) and displacement constraints, must be properly considered and are especially relevant in seismic applications (e.g., Ohtori *et al.* 2004) where the control devices are likely called to exert large dissipative forces that may lead to damages of the control system, loss of control effectiveness and phenomena of dynamic instability (Lim 2007).

*Corresponding author, Assistant Professor, E-mail: filippo.ubertini@unipg.it

Force saturation also affects semi-active devices, which are widely recognized today as the great promise of structural control (Casciati *et al.* 2006, Nagarajaiah and Narasimhan 2007) combining the reliability of passive devices (e.g., Symans *et al.* 2008, Casciati and Faravelli 2008, Casciati and Marzi 2010, Ubertini 2010) with the adaptability of active (e.g., Kobori *et al.* 1993, Reinhorn *et al.* 1993, Breccolotti *et al.* 2007, Ubertini 2008) and hybrid systems (e.g., Faravelli *et al.* 2010).

Magnetorheological (MR) dampers are perhaps the most widespread semi-active devices (e.g., Dyke *et al.* 1996, Renzi and Serino 2004), owing to their capability of exerting large dissipative control forces with low power requirements (Yang *et al.* 2002, Jung *et al.* 2003). Their force limitation directly derives from the limitation on the applicable voltage and is usually handled by means of “clipped optimal” and “modified clipped optimal” control strategies (Yoshida and Dyke 2004).

A quite general and powerful tool for handling a broad class of control system nonlinearities, including force saturation, is represented by the so-called “State-dependent Riccati Equation” (SDRE), early proposed by Cloutier (1997) and Friedland (1998). The method essentially consists of solving online (i.e., in real-time) the classic linear quadratic regulator problem (Panariello *et al.* 1997) with state-dependent weights and system matrices (Mracek and Cloutier 1998) in the spirit of adaptive control strategies (Narasimhan 2009, Nagarajaiah and Narasimhan 2010). Besides its conceptual simplicity, the main advantages of the SDRE with respect to well-known techniques are: (i) its applicability to different types of control devices; (ii) its ability to incorporate structural and control system non-linearities; (iii) its feasibility to handle a broad class of physical constraints, not limited to force saturation but also including, for instance, constraints on structural displacements. The last feature can be useful, for instance, in the case of limited strokes of inertial actuators and when performance limits are expressed in terms of maximum absolute displacements or maximum interstory drifts. Although it is true that the method is computationally demanding, its practical feasibility is somewhat guaranteed by the high performance computers available today in the market.

The application of the SDRE is not new in structural control. However, studies on this topic were essentially limited to active control and mainly focused on methods for choosing control weights on the basis of input severity. Basu and Nagarajaiah (2008), for instance, proposed to use wavelets for estimating the instantaneous frequency content of the seismic input and to consequently adapt the control weights. Although theoretical proofs of asymptotic stability and optimality are still missing in general cases (Erdem 2001), the effectiveness of the SDRE method and its robustness against random variations of system parameters are largely documented by means of simulation-based results (Beeler 2004).

The purpose of this paper is to present an alternative approach for designing saturation controllers for both active and semi-active systems using the SDRE. The work is a part of a research program recently started by the authors and concerning structural control strategies accounting for physical constraints. The first step of the research program was carried out in a recent paper (Materazzi and Ubertini 2012), where a non-linear SDRE-based controller was proposed for a structure equipped with one single active mass damper with force saturation and limited stroke. In the present paper the approach presented in (Materazzi and Ubertini 2012) is generalized to the use of multi-devices and to the presence of time delay, compensated by means of an appropriate technique. Moreover, a novel application of the SDRE in the context of semi-active control using MR dampers is proposed which results in a generalization of the well-established modified clipped optimal control strategy (Yoshida and Dyke 2004). The

effectiveness of the proposed approach is demonstrated by means of numerical simulations applied to a building case study which was already considered in the literature as a benchmark for comparing different seismic control solutions (Ohtori *et al.* 2004). In the numerical study, comparisons with existing saturation control techniques are carried out and the advantages of the proposed approach are discussed, as well.

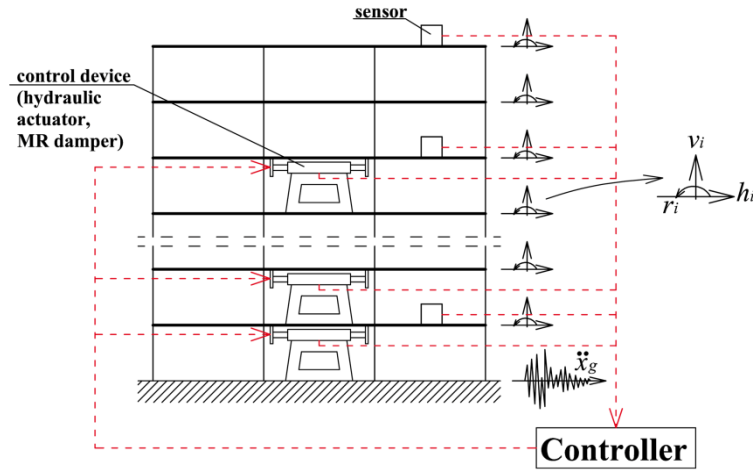


Fig. 1 Frame structure equipped with control devices

2. The method of the state dependent riccati equation

Let us consider a nonlinear dynamical system whose governing equation is expressed in pseudo-linear first-order form as follows

$$\dot{\mathbf{x}} = \mathbf{A}(\mathbf{x})\mathbf{x} + \mathbf{B}(\mathbf{x})\mathbf{u} \quad (1)$$

where \mathbf{x} is the state vector, $\mathbf{A}(\mathbf{x})$ and $\mathbf{B}(\mathbf{x})$ are state-dependent system matrices, \mathbf{u} is the vector of control forces and a dot denotes derivative with respect to time t .

In practice, control systems are designed to keep the structures in the linear range. Nonetheless, physical limitations of control devices make the equation of motion globally nonlinear. In order to apply the SDRE it is convenient to rewrite such equation in pseudo-linear form, as in Eq. (1), through direct parameterization.

The nonlinear regulator problem for the given system can be written in standard form as the minimization of the following performance index J

$$J = \frac{1}{2} \int_{t_0}^{\infty} (\mathbf{x}^T \mathbf{Q}(\mathbf{x}) \mathbf{x} + \mathbf{u}^T \mathbf{r}(\mathbf{x}) \mathbf{u}) dt \quad (2)$$

subjected to the constraint given by the equation of motion, Eq. (1), t_0 being a convenient initial time. In Eq. (2) the matrix \mathbf{Q} is a positive semi-definite state weight matrix and \mathbf{r} is a positive definite input weight matrix.

The SDRE is a very convenient tool for obtaining suboptimal solutions for the above-stated

problem. Essentially, the method consists of calculating the feedback control forces as

$$\mathbf{u} = -\mathbf{K}_u(\mathbf{x})\mathbf{x} = -\mathbf{r}^{-1}(\mathbf{x})\mathbf{B}^T(\mathbf{x})\mathbf{P}(\mathbf{x})\mathbf{x} \quad (3)$$

where $\mathbf{K}_u(\mathbf{x}) = \mathbf{r}^{-1}(\mathbf{x})\mathbf{B}^T(\mathbf{x})\mathbf{P}(\mathbf{x})$ is the state-dependent gain matrix and matrix $\mathbf{P}(\mathbf{x})$ solves the SDRE given by

$$\mathbf{A}^T(\mathbf{x})\mathbf{P} + \mathbf{P}\mathbf{A}(\mathbf{x}) - \mathbf{P}\mathbf{B}(\mathbf{x})\mathbf{r}^{-1}(\mathbf{x})\mathbf{B}^T(\mathbf{x})\mathbf{P} + \mathbf{Q}(\mathbf{x}) = \mathbf{0} \quad (4)$$

where $\mathbf{0}$ is the zero matrix with appropriate dimensions. As it can be recognized from Eqs. (3) and (4), the SDRE-based regulator is formally similar to the classic linear quadratic regulator (LQR) that applies to linear systems, but, in this case, all coefficient matrices are state dependent. As it is well-known (Cloutier 1997), the SDRE-based regulator satisfies the necessary conditions for the local asymptotic stability of the controlled system and asymptotically satisfies the necessary conditions for optimality of the solution.

3. Problem definition

Let us consider a plane frame structure with N stories, Fig. 1, subjected to ground acceleration \ddot{x}_g and protected by means of a control system consisting of interstory control devices (active or semi-active ones) with limited force capabilities. The forces exerted by the control devices are regulated by the controller using horizontal floor accelerations recorded by monitoring sensors as feedback information.

By applying a standard static condensation procedure the structure is modeled using three degrees of freedom for each story collected in the vector $\mathbf{q} = [h_1 \ v_1 \ r_1 \ h_2 \ v_2 \ r_2 \ \dots \ h_N \ v_N \ r_N]^T$, h_i , v_i and r_i being the horizontal displacement, the vertical displacement and the in-plane rotation of the i -th story, respectively.

The equation of motion of this structure subjected to seismic excitation and equipped with m control devices is written as follows

$$\mathbf{M}\ddot{\mathbf{q}} + \mathbf{C}\dot{\mathbf{q}} + \mathbf{K}\mathbf{q} = -\mathbf{M}\{\mathbf{1}\}\ddot{x}_g + \mathbf{F}\mathbf{u} \quad (5)$$

where \mathbf{M} , \mathbf{C} and \mathbf{K} are the $n \times n$ mass, damping and stiffness matrices, respectively, with $n = 3N$, \mathbf{u} is the m -dimensional vector of control forces and $\{\mathbf{1}\}$ and \mathbf{F} are convenient collocation vectors, with $n \times 1$ and $n \times m$ dimensions, respectively.

In seismic applications interstory drifts are perhaps more significant parameters than absolute floor displacements. Hence, a coordinate vector, ξ , containing interstory drifts as Lagrangian parameters is conveniently introduced and defined as $\xi = [h_1 \ v_1 \ r_1 \ h_2 - h_1 \ v_2 \ r_2 \ \dots \ h_N - h_{N-1} \ v_N \ r_N]^T$. Then, a change of coordinates from \mathbf{q} to ξ by means of the following linear transformation is carried out

$$\begin{bmatrix} \mathbf{q} \\ \dot{\mathbf{q}} \end{bmatrix} = \mathbf{R} \begin{bmatrix} \xi \\ \dot{\xi} \end{bmatrix} \quad (6)$$

where \mathbf{R} is the transformation matrix.

$$\begin{bmatrix} \ddot{\xi} \\ \dot{\xi} \\ \xi \end{bmatrix} = \mathbf{R}^{-1} \begin{bmatrix} \mathbf{0}_{n \times n} & \mathbf{I}_{n \times n} \\ -\mathbf{M}^{-1}\mathbf{K} & -\mathbf{M}^{-1}\mathbf{C} \end{bmatrix} \mathbf{R} \begin{bmatrix} \xi \\ \dot{\xi} \\ \ddot{\xi} \end{bmatrix} + \mathbf{R}^{-1} \begin{bmatrix} \mathbf{0}_{n \times 1} \\ \mathbf{M}^{-1}\mathbf{F} \end{bmatrix} \mathbf{u} + \mathbf{R}^{-1} \begin{bmatrix} \mathbf{0}_{n \times 1} \\ -\{\mathbf{1}\} \end{bmatrix} \ddot{x}_g \quad (7)$$

where $\mathbf{0}_{n \times n}$ and $\mathbf{I}_{n \times n}$ are the zero and identity matrices with dimensions $n \times n$, respectively.

Eq. (7) is the first order equation of the system in transformed coordinates. By defining the state vector \mathbf{x} as $\mathbf{x} = [\xi \quad \dot{\xi}]^T$, the following synthetic form of Eq. (7) is obtained

$$\dot{\mathbf{x}} = \mathbf{A}\mathbf{x} + \mathbf{B}\mathbf{u} + \mathbf{G}\ddot{x}_g \quad (8)$$

with obvious definitions of matrices \mathbf{A} , \mathbf{B} and \mathbf{G} .

4. Proposed saturation control algorithm

4.1 Active bracing system

First of all we consider the case where the m control devices, in Fig. 1, are generic actuators able to exert maximum forces equal to $u_{\max,1}$, $u_{\max,2}$, ..., $u_{\max,m}$. In order to account for their force saturation, the following equation is introduced

$$\mathbf{u} = \mathbf{u}_{\text{sat}}(\mathbf{z}) = \begin{bmatrix} u_{\max,1} \cdot \varepsilon(z_1) \\ u_{\max,2} \cdot \varepsilon(z_2) \\ \vdots \\ u_{\max,m} \cdot \varepsilon(z_m) \end{bmatrix} \quad (9)$$

which links the vector of control forces \mathbf{u} to m additional variables z_1, z_2, \dots, z_m , collected in the vector $\mathbf{z} = [z_1 \quad z_2 \quad \dots \quad z_m]^T$, choosing an expression for the saturation function $\varepsilon(\bullet)$ which does not violate the physical constraint. In this work the following expression is adopted for this purpose

$$\varepsilon(s) = \begin{cases} -1 & \text{if } s < -k_1 \frac{\pi}{2} \\ \sin\left(\frac{s}{k_1}\right) & \text{if } -k_1 \frac{\pi}{2} \leq s \leq k_1 \frac{\pi}{2} \\ 1 & \text{if } s > k_1 \frac{\pi}{2} \end{cases} \quad (10)$$

whose plot is shown in Fig. 2(a).

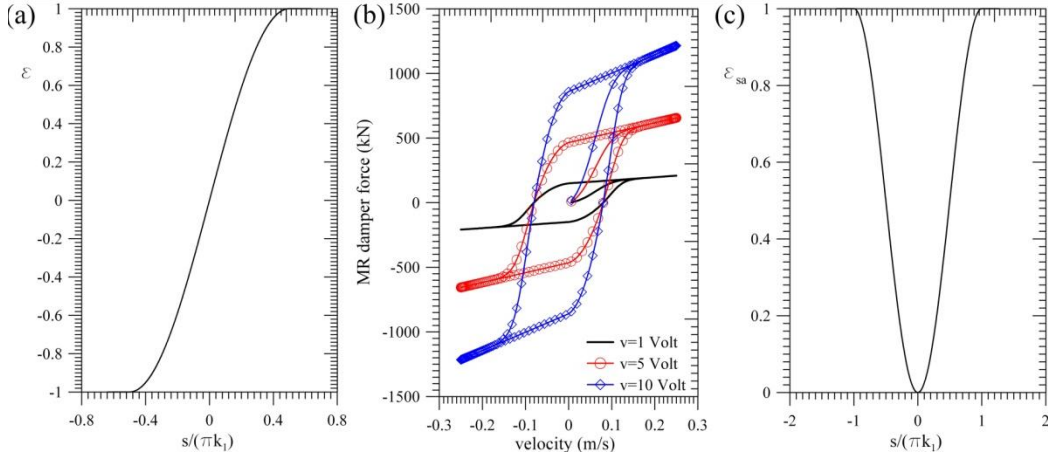


Fig. 2 (a) Saturation function ε , (b) typical force-velocity responses of a MR damper and (c) saturation function ε_{sa}

After introducing Eqs. (9) and (10) into Eq. (8), an additional equation is needed in order to make the system controllable. To this end, the following one is here adopted

$$\dot{\mathbf{z}} = \mathbf{u}_1 \quad (11)$$

where \mathbf{u}_1 is a m -dimensional vector of pseudo-control inputs to be regulated by the controller. Making use of Eqs. (9)-(11), the equation of motion, Eq. (8), is written in terms of augmented state as

$$\begin{bmatrix} \dot{\mathbf{x}} \\ \dot{\mathbf{z}} \end{bmatrix} = \begin{bmatrix} \mathbf{A} & \mathbf{B} \cdot \mathbf{U}_{sat}(\mathbf{z}) \\ \mathbf{0}_{m \times 2n} & \mathbf{0}_{m \times m} \end{bmatrix} \begin{bmatrix} \mathbf{x} \\ \mathbf{z} \end{bmatrix} + \begin{bmatrix} \mathbf{0}_{2n \times m} \\ \mathbf{I}_{m \times m} \end{bmatrix} \mathbf{u}_1 + \begin{bmatrix} \mathbf{G} \\ \mathbf{0}_{m \times 1} \end{bmatrix} \ddot{x}_g \quad (12)$$

where matrix \mathbf{U}_{sat} is defined as

$$\mathbf{U}_{sat} = \begin{bmatrix} \frac{u_{\max,1} \varepsilon(z_1)}{z_1} & 0 & \dots & 0 \\ 0 & \frac{u_{\max,2} \varepsilon(z_2)}{z_2} & & \vdots \\ \vdots & & \ddots & 0 \\ 0 & \dots & 0 & \frac{u_{\max,m} \varepsilon(z_m)}{z_m} \end{bmatrix} \quad (13)$$

Eq. (12) possesses the same mathematical structure of Eq. (1). Therefore, the pseudo-control feedback \mathbf{u}_1 can be regulated using the SDRE, likewise in Eq. (3), as follows

$$\mathbf{u}_1 = -\mathbf{K}_{u1}(\mathbf{x}, \mathbf{z}) \begin{bmatrix} \mathbf{x} \\ \mathbf{z} \end{bmatrix} = -\begin{bmatrix} \mathbf{K}_{u1,x}(\mathbf{x}, \mathbf{z}) & \mathbf{K}_{u1,z}(\mathbf{x}, \mathbf{z}) \end{bmatrix} \begin{bmatrix} \mathbf{x} \\ \mathbf{z} \end{bmatrix} \quad (14)$$

where $\mathbf{K}_{u1} = \begin{bmatrix} \mathbf{K}_{u1,x} & \mathbf{K}_{u1,z} \end{bmatrix}$ is the state-dependent gain matrix calculated according to Eq. (4).

4.2 Semi-active bracing system using MR dampers

The method proposed in Section 4.1 can be readily extended to semi-active MR dampers with voltage constraints. To this end, it is necessary to introduce an appropriate mathematical model to describe the hysteretic behavior of the MR dampers. The classic Bouc-Wen model can be effectively employed for this purpose (Yung *et al.* 2003). Accordingly, the control force u_i exerted by the i -th MR damper can be expressed as

$$u_i = \alpha_i z_i^* + c_{0,i} (\dot{h}_i - \dot{h}_{i-1}) \quad (15)$$

where z_i^* is an evolutionary variable obeying the Bouc-Wen equation (e.g., Yoshida and Dyke 2004)

$$\dot{z}_i^* = -\gamma |\dot{h}_i - \dot{h}_{i-1}| z_i^* z_i^{*\bar{n}-1} - \beta (\dot{h}_i - \dot{h}_{i-1}) |z_i^*|^{\bar{n}} + A_{MR} (\dot{h}_i - \dot{h}_{i-1}) \quad (16)$$

The parameters α_i and $c_{0,i}$ appearing in Eq. (15) can be varied by regulating the applied voltage v_i . In fact, the functional dependencies of α_i and $c_{0,i}$ on v_i can be modeled as

$$\begin{aligned} \alpha_i &= \alpha_a + \alpha_b v_i \\ c_{0,i} &= c_{0a} + c_{0b} v_i \end{aligned} \quad (17)$$

In Eqs. (15)-(17), α_a , α_b , c_{0a} , c_{0b} , γ , β , \bar{n} and A_{MR} are parameters which characterize the MR damper (Yoshida and Dyke 2004). As examples, the force-velocity responses of a typical 1000-kN MR damper are depicted in Fig. 2(b) where the parameters reported by Jung *et al.* (2003) have been used.

Eqs. (15) and (16) are conveniently rewritten in matrix form as follows

$$\begin{aligned} \mathbf{u} &= \mathbf{f}_u(\mathbf{x}, \mathbf{z}^*) \mathbf{v} \\ \dot{\mathbf{z}}^* &= \mathbf{f}_z(\mathbf{x}, \mathbf{z}^*) \mathbf{z}^* \end{aligned} \quad (18)$$

where $\mathbf{v} = [v_1 \ v_2 \ \dots \ v_m]^T$ and $\mathbf{z}^* = [z_1^* \ z_2^* \ \dots \ z_m^*]^T$, while the definitions of $\mathbf{f}_u(\mathbf{x}, \mathbf{z}^*)$ and $\mathbf{f}_z(\mathbf{x}, \mathbf{z}^*)$ are implicit from Eqs. (15)-(17).

It should be noticed that matrix $\mathbf{f}_u(\mathbf{x}, \mathbf{z}^*)$, in Eq. (18), contains the values of the semi-active control forces exerted by the MR dampers. Hence, a load cell for each semi-active device is necessary to measure such quantities.

The voltages applied to the m MR dampers cannot exceed maximum values $V_{\max,1}$, $V_{\max,2}$, \dots , $V_{\max,m}$. To account for these constraints, a strategy similar to that proposed in Section 4.1 can be

applied. To this end, the following two equations are introduced

$$\mathbf{v} = \mathbf{v}_{sat}(\mathbf{z}) = \begin{bmatrix} V_{\max,1} \varepsilon_{sa}(z_1) \\ V_{\max,2} \varepsilon_{sa}(z_2) \\ \vdots \\ V_{\max,m} \varepsilon_{sa}(z_m) \end{bmatrix} \quad (19)$$

$$\dot{\mathbf{z}} = \mathbf{u}_1 \quad (20)$$

where the voltages appear as slave controlled variables and where $\varepsilon_{sa}(\bullet)$ is defined as follows

$$\varepsilon_{sa}(s) = \begin{cases} 1 & \text{if } |s| > k_1 \pi \\ \frac{1}{2} \left(\sin \left(\frac{s}{k_1} - \frac{\pi}{2} \right) + 1 \right) & \text{if } |s| \leq k_1 \pi \end{cases} \quad (21)$$

whose plot is shown in Fig. 2(c). Noticeably, since voltages can only assume positive values, the chosen expression for the saturation function $\varepsilon_{sa}(\bullet)$ is always positive. After introducing Eqs. (18)-(21), the equation of motion becomes the following

$$\begin{bmatrix} \dot{\mathbf{x}} \\ \dot{\mathbf{z}} \end{bmatrix} = \begin{bmatrix} \mathbf{A} & \mathbf{B}\mathbf{f}_u(\mathbf{x}, \mathbf{z}^*) \mathbf{V}_{sat} \\ \mathbf{0}_{m \times 2n} & \mathbf{0}_{m \times m} \end{bmatrix} \begin{bmatrix} \mathbf{x} \\ \mathbf{z} \end{bmatrix} + \begin{bmatrix} \mathbf{G} \\ \mathbf{0}_{m \times 1} \end{bmatrix} \ddot{x}_g + \begin{bmatrix} \mathbf{0}_{2n \times m} \\ \mathbf{I}_{m \times m} \end{bmatrix} \mathbf{u}_1 \quad (22)$$

where the time evolution of the variables contained in vector \mathbf{z}^* is governed by the second expression in Eq. (18) and matrix \mathbf{V}_{sat} is defined as

$$\mathbf{V}_{sat} = \begin{bmatrix} \frac{V_{\max,1} \varepsilon(z_1)}{z_1} & 0 & \dots & 0 \\ 0 & \frac{V_{\max,2} \varepsilon(z_2)}{z_2} & & \vdots \\ \vdots & & \ddots & 0 \\ 0 & \dots & 0 & \frac{V_{\max,m} \varepsilon(z_m)}{z_m} \end{bmatrix} \quad (23)$$

Eq. (22) is equivalent to Eq. (12). Therefore, the pseudo-control feedback \mathbf{u}_1 can be regulated using the SDRE, as in Eq. (14).

4.3 Controller design

Looking at the previous derivations, the equation of motion of the active and semi-active saturation systems assume the same mathematical structure, which is the following one

$$\begin{aligned} \dot{\mathbf{x}} &= \mathbf{A}\mathbf{x} + \mathbf{B} \cdot \Theta(\mathbf{z}) \cdot \mathbf{z} + \mathbf{G}\ddot{x}_g \\ \dot{\mathbf{z}} &= \mathbf{u}_1 \end{aligned} \tag{24}$$

where Θ is equal to

$$\Theta(\mathbf{z}) = \begin{cases} \mathbf{U}_{sat}(\mathbf{z}) & \text{activecase} \\ \mathbf{f}_u(\mathbf{x}, \mathbf{z}^*) \mathbf{V}_{sat}(\mathbf{z}) & \text{semi-activecase} \end{cases} \tag{25}$$

In both cases the control forces can be written as

$$\mathbf{u} = \Theta(\mathbf{z})\mathbf{z} \tag{26}$$

In order to apply the SDRE it is necessary to choose the control weights that define the performance index, J , in Eq. (2). In this work, J is chosen as follows

$$J = \frac{1}{2} \int_{t_0}^{\infty} \sum_{i=1}^n (Q_i q_i^2 + Q_{n+i} \dot{q}_i^2) + \sum_{i=1}^m r_i u_i^2 dt \tag{27}$$

where the penalizations Q_i and r_i are applied to the structural degrees of freedom q_i and to their first derivatives \dot{q}_i , as well as to the control forces u_i . However, the SDRE requires such penalizations to be applied to the state variables x_i (structural degrees of freedom expressed in transformed coordinates and their time derivatives), to the internal variables z_i and to the pseudo-control input \mathbf{u}_1 . Therefore, it is necessary to derive an expression of J which is equivalent to Eq. (27), but written in the appropriate form. This can be done by substituting Eqs. (6) and (26) into Eq. (27). After straightforward computations, the following synthetic form of the J index is obtained

$$J = \frac{1}{2} \int_{t_0}^{\infty} \left(\begin{bmatrix} \mathbf{x} \\ \mathbf{z} \end{bmatrix}^T \bar{\mathbf{Q}}(\mathbf{x}, \mathbf{z}) \begin{bmatrix} \mathbf{x} \\ \mathbf{z} \end{bmatrix} + \mathbf{u}_1^T \mathbf{r}_1 \mathbf{u}_1 \right) dt \tag{28}$$

with

$$\bar{\mathbf{Q}}(\mathbf{x}, \mathbf{z}) = \begin{bmatrix} \mathbf{R}^T \begin{bmatrix} Q_1 & 0 & \dots & 0 \\ 0 & Q_2 & & \vdots \\ \vdots & & \ddots & 0 \\ 0 & \dots & 0 & Q_{2n} \end{bmatrix} \mathbf{R} & \mathbf{0}_{2n \times m} \\ \mathbf{0}_{m \times 2n} & \begin{bmatrix} r_1 \Theta_{11}^2 & 0 & \dots & 0 \\ 0 & r_2 \Theta_{22}^2 & & \vdots \\ \vdots & & \ddots & 0 \\ 0 & \dots & 0 & r_m \Theta_{mm}^2 \end{bmatrix} \end{bmatrix} \tag{29}$$

where Θ_{ii} is the i -th term contained along the main diagonal of matrix Θ , Eq. (25), and \mathbf{r}_1 is a

diagonal matrix that contains small penalties $r_{1,i}$, $i = 1, 2, \dots, m$, applied to the components of the pseudo control input \mathbf{u}_1 and necessary to avoid a singular problem.

It should be noticed that the proposed approach could be generalized by introducing additional state dependent terms in Eq. (29). Although this would go beyond the purposes of the present study, it is worth mentioning that a similar approach might be useful to penalize the interstory drifts when approaching their performance limits. This task is indeed facilitated by the use of interstory drifts as state variables.

4.4 Time delay compensation and state reconstruction

In both active and semi-active cases the vector of control forces depends upon the additional state variables contained in the vector \mathbf{z} . Because these quantities are internal variables the physical actuation is delayed of a quantity τ . Moreover, since the solution of the SDRE requires time-consuming operations, it cannot be continuously computed. On the contrary, the SDRE can be practically solved and the gain matrix can be updated every discrete time interval of length τ_{SDRE} .

In this paper, a time delay compensation is considered for mitigating the effects of time delay τ . On the contrary, τ_{SDRE} is accounted for, but not compensated.

Time delay compensation is here performed by applying the procedure described by Soong (1990) which is based on the introduction of $\mathbf{z}_2 \cong \mathbf{z}(t - \tau)$ and $\mathbf{z}_3 \cong \dot{\mathbf{z}}(t - \tau)$ as additional state variables. After straightforward computations, not reported here for the sake of brevity, the following equation of motion is obtained in terms of augmented state

$$\begin{bmatrix} \dot{\mathbf{x}} \\ \dot{\mathbf{z}} \\ \dot{\mathbf{z}}_2 \\ \dot{\mathbf{z}}_3 \end{bmatrix} = \begin{bmatrix} \mathbf{A} & \mathbf{0}_{2n \times m} & \mathbf{B} \cdot \Theta(\mathbf{z}(t - \tau_{SDRE})) & \mathbf{0}_{2n \times m} \\ \mathbf{0}_{m \times 2n} & \mathbf{0}_{m \times m} & \mathbf{0}_{m \times m} & \mathbf{0}_{m \times m} \\ \mathbf{0}_{m \times 2n} & \mathbf{0}_{m \times m} & \mathbf{0}_{m \times m} & \mathbf{I}_{m \times m} \\ \mathbf{0}_{m \times 2n} & \frac{2}{\tau^2} \cdot \mathbf{I}_{m \times m} & -\frac{2}{\tau} \cdot \mathbf{I}_{m \times m} & -\frac{2}{\tau} \cdot \mathbf{I}_{m \times m} \end{bmatrix} \begin{bmatrix} \mathbf{x} \\ \mathbf{z} \\ \mathbf{z}_2 \\ \mathbf{z}_3 \end{bmatrix} + \begin{bmatrix} \mathbf{0}_{2n \times m} \\ \mathbf{I}_{m \times m} \\ \mathbf{0}_{m \times m} \\ \mathbf{0}_{m \times m} \end{bmatrix} \mathbf{u}_1 + \begin{bmatrix} \mathbf{G} \\ \mathbf{0}_{m \times 1} \\ \mathbf{0}_{m \times 1} \\ \mathbf{0}_{m \times 1} \end{bmatrix} \ddot{\mathbf{x}}_g \quad (30)$$

where the dependence of the control forces on the delayed quantities $\mathbf{z}(t - \tau_{SDRE})$ and $\mathbf{z}(t - \tau)$ should be noticed. The state dependent feedback pseudo-control input \mathbf{u}_1 can now be calculated using the SDRE by considering the augmented system matrices in Eq. (30). By doing so, the following equation is obtained:

$$\mathbf{u}_1 = -\mathbf{K}_{u1}^\tau(\mathbf{x}, \mathbf{z}, \mathbf{z}_2, \mathbf{z}_3) \begin{bmatrix} \mathbf{x} \\ \mathbf{z} \\ \mathbf{z}_2 \\ \mathbf{z}_3 \end{bmatrix} = -\begin{bmatrix} \mathbf{K}_{u1,x}^\tau & \mathbf{K}_{u1,z}^\tau & \mathbf{K}_{u1,z2}^\tau & \mathbf{K}_{u1,z3}^\tau \end{bmatrix} \begin{bmatrix} \mathbf{x} \\ \mathbf{z} \\ \mathbf{z}_2 \\ \mathbf{z}_3 \end{bmatrix} \quad (31)$$

In practical implementations of the proposed procedure it should be also considered that the actual value of the state vector in Eq. (31) is unknown, and should be estimated using the measured variables. In this work absolute horizontal floor accelerations are used for this purpose

(Fig. 1) and conveniently collected in a vector \mathbf{y} that is defined as $\mathbf{y} = \mathbf{C}_a (\ddot{\mathbf{q}} + \{1\} \ddot{x}_g)$, \mathbf{C}_a being the selection matrix. After straightforward computations, vector \mathbf{y} can be expressed as a function of the state variables of the system in the following form

$$\mathbf{y} = -\mathbf{C}_a \left[\mathbf{M}^{-1} \mathbf{K} \quad \mathbf{M}^{-1} \mathbf{C} \right] \mathbf{R} \mathbf{x} + \mathbf{C}_a \mathbf{M}^{-1} \mathbf{F} \mathbf{u} = \mathbf{C} \mathbf{x} + \mathbf{D} \mathbf{u} \quad (32)$$

with obvious definitions of matrices \mathbf{C} and \mathbf{D} . Then, an estimate $\hat{\mathbf{x}}$ of the state is obtained by means of a standard Kalman's observer. The equations governing the physical system and the state observer can thus be written in the following synthetic form

$$\begin{bmatrix} \dot{\hat{\mathbf{x}}} \\ \dot{\hat{\mathbf{x}}} \\ \dot{\mathbf{z}} \\ \dot{\mathbf{z}}_2 \\ \dot{\mathbf{z}}_3 \end{bmatrix} = \begin{bmatrix} \mathbf{A} & \mathbf{0}_{2n \times 2n} & \mathbf{0}_{2n \times m} & \mathbf{B} \cdot \Theta(\mathbf{z}(t - \tau_{SDRE})) & \mathbf{0}_{2n \times m} \\ \mathbf{L} \mathbf{C} & \mathbf{A} - \mathbf{L} \mathbf{C} & \mathbf{0}_{2n \times m} & \mathbf{B} \cdot \Theta(\mathbf{z}(t - \tau_{SDRE})) & \mathbf{0}_{2n \times m} \\ \mathbf{0}_{m \times 2n} & -\mathbf{K}_{u1,x}^\tau & -\mathbf{K}_{u1,z}^\tau & -\mathbf{K}_{u1,z2}^\tau & -\mathbf{K}_{u1,z3}^\tau \\ \mathbf{0}_{m \times 2n} & \mathbf{0}_{m \times 2n} & \mathbf{0}_{m \times m} & \mathbf{0}_{m \times m} & \mathbf{I}_{m \times m} \\ \mathbf{0}_{m \times 2n} & \mathbf{0}_{m \times 2n} & \frac{2}{\tau^2} \cdot \mathbf{I}_{m \times m} & -\frac{2}{\tau^2} \cdot \mathbf{I}_{m \times m} & -\frac{2}{\tau} \cdot \mathbf{I}_{m \times m} \end{bmatrix} \begin{bmatrix} \mathbf{x} \\ \hat{\mathbf{x}} \\ \mathbf{z} \\ \mathbf{z}_2 \\ \mathbf{z}_3 \end{bmatrix} + \begin{bmatrix} \mathbf{G} \\ \mathbf{0}_{2n \times 1} \\ \mathbf{0}_{m \times 1} \\ \mathbf{0}_{m \times 1} \\ \mathbf{0}_{m \times 1} \end{bmatrix} \ddot{x}_g \quad (33)$$

\mathbf{L} being Kalman's filter gain matrix. In this way, a saturation controller for both active and semi-active systems using acceleration feedback with time delay compensation and state reconstruction has been obtained.

5. Numerical example

5.1 Characteristics of the structure

The case study chosen in this work is represented by a 9-stories steel building already adopted in the literature (Ohtori *et al.* 2004) as a benchmark for evaluating the effectiveness of different control strategies. The building is square in plan, with 45.7 x 45.7 m dimensions, and 37.2 m in elevation. The seismic resisting system is comprised of steel perimeter moment frames (MFs) with 5 bays. The interior frames are built using simple beam-column connections. The beams act compositely with the floor slabs and each MF resists one half of the total seismic load in each direction. The total seismic mass is equal to 9000 tons. The first ten natural frequencies of the structure are: 0.468, 1.235, 2.136, 3.211, 4.404, 5.339, 5.787, 7.107, 8.380 and 10.153 Hz. Additional details can be found in (Ohtori *et al.* 2004).

5.2 Analysis procedure

El Centro, Kobe and Northridge seismic records, scaled at different values of the peak ground acceleration (PGA), are considered in the numerical simulations. In particular, in order to test the effectiveness of the proposed approach in presence of extreme seismic events, a maximum PGA of 0.60 g is considered in the analysis.

Because the equation of motion is expressed in pseudo-linear form, it is solved by means of a numerical procedure that considers a series of linear systems whose matrices are updated every

time step of length τ_{SDRE} , where τ_{SDRE} , as already mentioned, is the time step chosen for solving the SDRE. Within the generic time interval $[t \ t + \tau_{SDRE}]$ the system, governed by Eq. (33), is locally linear and its solution is calculated using the instantaneous value of the transfer function and the results at time t as initial conditions. In the analysis, τ_{SDRE} is assumed to be equal to 0.02 sec, while τ is assumed to be equal to 0.005 s.

In order to perform a quantitative evaluation of the control performances, eight evaluation criteria, J_1, J_2, \dots, J_8 , are considered and summarized in Table 1. In such a table the superscript 0 indicates the uncontrolled solution, H_i is the i -th interstory height, V_b and V_b^0 are the base shear with and without control, respectively, the norm $\|\ast\|$ represents the root mean square operator and u_{\max} is the reference maximum force capacity of the control devices equal to 1000 kN. It is worthwhile to note that J_8 , defined in Table 1, measures the peak power required by the control system normalized to the value, W_{\max} , required by the ideal LQR strategy at a PGA of 0.60 g .

Table 1 Performance indices of control effectiveness

Peak interstory drift	Peak floor acceleration	Peak base shear	RMS interstory drift
$J_1 = \frac{\max_{t,i} \frac{ h_i - h_{i-1} }{H_i}}{\max_{t,i} \frac{ h_i^0 - h_{i-1}^0 }{H_i}}$	$J_2 = \frac{\max_{t,i} \ddot{q}_{ai} }{\max_{t,i} \ddot{q}_{ai}^0 }$	$J_3 = \frac{\max_t V_b }{\max_t V_b^0 }$	$J_4 = \frac{\max_i \frac{\ h_i - h_{i-1}\ }{H_i}}{\max_i \frac{\ h_i^0 - h_{i-1}^0\ }{H_i}}$
RMS floor acceleration	RMS base shear	Peak control force	Peak control power
$J_5 = \frac{\max_i \ \ddot{x}_g + \ddot{q}_i\ }{\max_i \ \ddot{x}_g + \ddot{q}_i^0\ }$	$J_6 = \frac{\ V_b\ }{\ V_b^0\ }$	$J_7 = \frac{\max_{t,i} u_i }{u_{\max}}$	$J_8 = \frac{\max_t \sum_i (\dot{h}_i - \dot{h}_{i-1}) u_i }{W_{\max}}$

5.3 Active control strategy with force saturation

The effectiveness of the SDRE-based active saturation control strategy for different values of the PGA is investigated at first. The structure is controlled using nine actuators, one for each interstory, with maximum force capacities u_{\max} of 1000 kN each. Servo-controlled hydraulic actuators which such a capacity can be readily raised in the market.

Parameter k_f , appearing in Eq. (10), was chosen in the analysis as 10^3 . This value is strictly related to the rate of force saturation and was chosen to be sufficiently large that significant

impulsive excitation components did not arise when force saturation occurred, thus not limiting control effectiveness in mitigating floor accelerations. Unitary state weight parameters Q_1, Q_2, \dots, Q_{2n} were adopted in Eq. (29), while weights on control forces r_1, r_2, \dots, r_m were assumed equal to $2 \cdot 10^{-14}$. The quantities $r_{1,i}$ in Eq. (28) were chosen equal to 10^{-17} and online increased to 10^{-10} during the motion after the occurrence of the first force saturation.

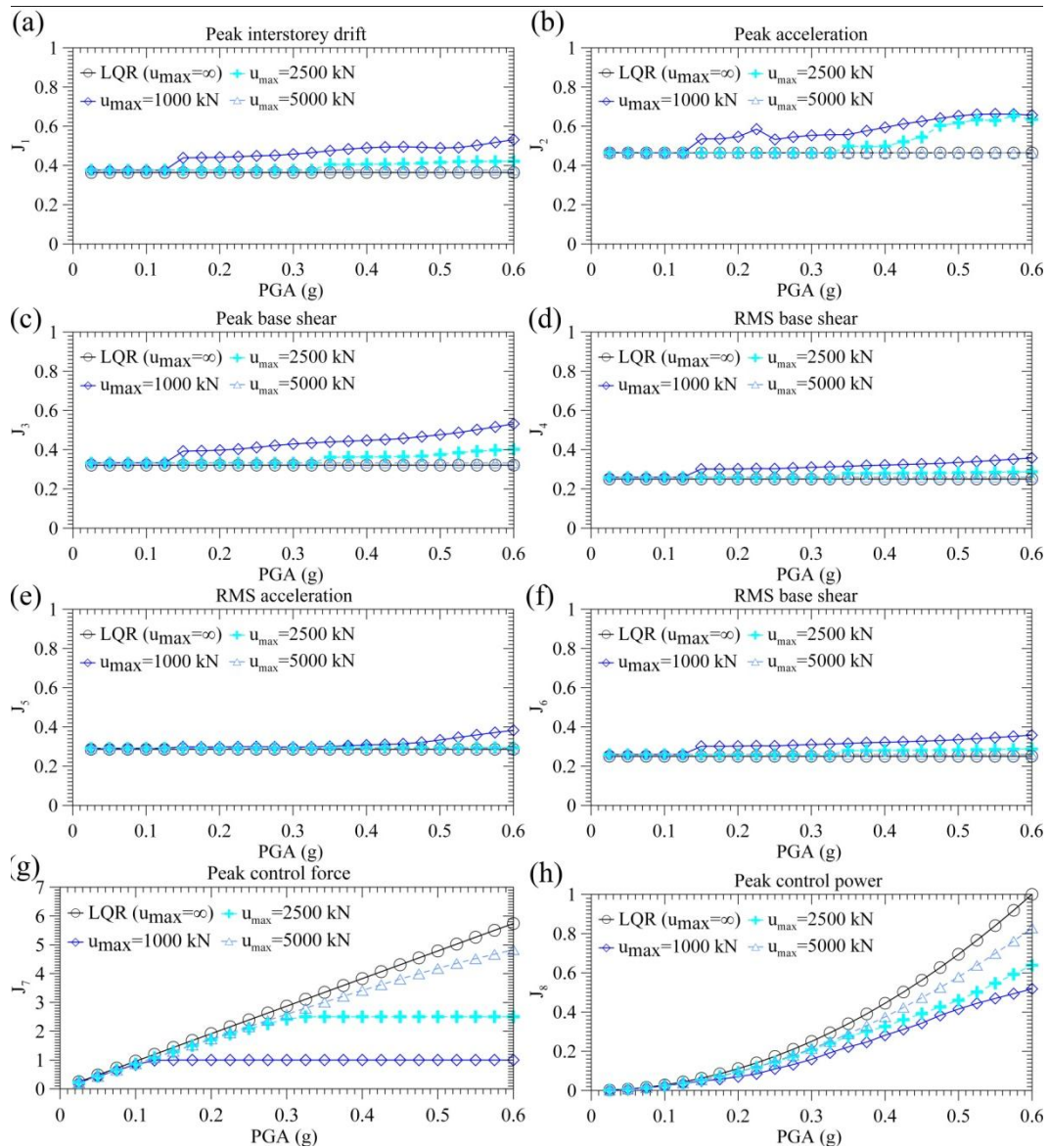


Fig. 3 Active control under El Centro ground motion: performance of ideal LQR system, saturation system with $u_{\max}=1000$ kN, saturation system with $u_{\max}=2500$ kN, saturation system with $u_{\max}=5000$ kN

Fig. 3 shows the variations of the eight evaluation criteria for a PGA up to 0.60 g in the case of the El Centro ground motion. The results concerning Kobe and Northridge earthquakes are presented in Table 2. For providing reference values, the performances of the SDRE-based control system with 1000 kN actuators are compared with those of the ideal LQR case without actuators' saturation nor time delay, as well as with those of the saturation cases with 2500 kN and 5000 kN actuators. The ideal LQR controller was constructed using the same weights Q_1, Q_2, \dots, Q_{2n} and r_1, r_2, \dots, r_m adopted for the SDRE-based approach.

Table 2 Active control under Kobe and Northridge ground motions: performance of ideal LQR system, and saturation systems with $u_{\max}=1000$ kN, $u_{\max}=2500$ kN and $u_{\max}=5000$ kN

PGA (g)		Kobe						Northridge					
		0.1	0.2	0.3	0.4	0.5	0.6	0.1	0.2	0.3	0.4	0.5	0.6
J ₁	LQR	0.47	0.47	0.47	0.47	0.47	0.47	0.43	0.43	0.43	0.43	0.43	0.43
	$u_{\max}=1000$ kN	0.53	0.59	0.75	0.79	0.80	0.83	0.55	0.58	0.64	0.66	0.67	0.68
	$u_{\max}=2500$ kN	0.48	0.48	0.49	0.53	0.57	0.66	0.45	0.45	0.50	0.52	0.57	0.60
	$u_{\max}=5000$ kN	0.48	0.48	0.48	0.48	0.48	0.49	0.45	0.45	0.45	0.45	0.48	0.49
J ₂	LQR	0.45	0.45	0.45	0.45	0.45	0.45	0.37	0.37	0.37	0.37	0.37	0.37
	$u_{\max}=1000$ kN	0.53	0.65	0.92	0.97	0.98	0.97	0.37	0.41	0.56	0.68	0.73	0.77
	$u_{\max}=2500$ kN	0.46	0.51	0.71	0.74	0.67	0.81	0.37	0.37	0.37	0.37	0.43	0.48
	$u_{\max}=5000$ kN	0.46	0.46	0.46	0.53	0.71	0.81	0.37	0.37	0.37	0.37	0.37	0.37
J ₃	LQR	0.47	0.47	0.47	0.47	0.47	0.47	0.31	0.31	0.31	0.31	0.31	0.31
	$u_{\max}=1000$ kN	0.54	0.60	0.68	0.73	0.78	0.81	0.39	0.43	0.42	0.45	0.54	0.61
	$u_{\max}=2500$ kN	0.48	0.48	0.49	0.54	0.58	0.61	0.33	0.33	0.37	0.40	0.42	0.42
	$u_{\max}=5000$ kN	0.48	0.48	0.48	0.48	0.48	0.47	0.33	0.33	0.33	0.33	0.34	0.37
J ₄	LQR	0.27	0.27	0.27	0.27	0.27	0.27	0.22	0.22	0.22	0.22	0.22	0.22
	$u_{\max}=1000$ kN	0.32	0.36	0.41	0.44	0.48	0.51	0.26	0.29	0.33	0.37	0.41	0.45
	$u_{\max}=2500$ kN	0.28	0.29	0.30	0.32	0.35	0.37	0.23	0.23	0.24	0.25	0.27	0.29
	$u_{\max}=5000$ kN	0.28	0.28	0.28	0.29	0.29	0.29	0.23	0.23	0.23	0.23	0.23	0.23
J ₅	LQR	0.33	0.33	0.33	0.33	0.33	0.33	0.30	0.30	0.30	0.30	0.30	0.30
	$u_{\max}=1000$ kN	0.33	0.35	0.44	0.48	0.52	0.56	0.30	0.30	0.33	0.38	0.43	0.47
	$u_{\max}=2500$ kN	0.33	0.34	0.34	0.33	0.35	0.38	0.31	0.31	0.31	0.31	0.31	0.30
	$u_{\max}=5000$ kN	0.33	0.33	0.33	0.34	0.34	0.34	0.31	0.31	0.31	0.31	0.31	0.31
J ₆	LQR	0.31	0.31	0.31	0.31	0.31	0.31	0.30	0.30	0.30	0.30	0.30	0.30
	$u_{\max}=1000$ kN	0.36	0.39	0.41	0.42	0.44	0.47	0.34	0.37	0.39	0.40	0.43	0.45
	$u_{\max}=2500$ kN	0.32	0.34	0.35	0.36	0.38	0.38	0.31	0.31	0.33	0.35	0.36	0.37
	$u_{\max}=5000$ kN	0.32	0.32	0.32	0.33	0.34	0.34	0.31	0.31	0.31	0.31	0.32	0.32
J ₇	LQR	1.51	3.01	4.52	6.03	7.53	9.04	1.22	2.44	3.66	4.88	6.10	7.32
	$u_{\max}=1000$ kN	1.00	1.00	1.00	1.00	1.00	1.00	1.00	1.00	1.00	1.00	1.00	1.00
	$u_{\max}=2500$ kN	1.45	2.50	2.50	2.50	2.50	2.50	1.15	2.26	2.50	2.50	2.50	2.50
	$u_{\max}=5000$ kN	1.45	2.90	4.32	5.00	5.00	5.00	1.16	2.31	3.43	4.53	5.00	5.00
J ₈	LQR	0.03	0.11	0.25	0.44	0.69	1.00	0.03	0.11	0.25	0.44	0.69	1.00
	$u_{\max}=1000$ kN	0.03	0.09	0.14	0.19	0.23	0.28	0.03	0.07	0.14	0.21	0.29	0.37
	$u_{\max}=2500$ kN	0.03	0.10	0.20	0.34	0.56	0.71	0.03	0.11	0.20	0.32	0.43	0.58
	$u_{\max}=5000$ kN	0.03	0.11	0.25	0.42	0.61	0.77	0.03	0.11	0.24	0.42	0.64	0.83

Because the ideal LQR system is linear, the corresponding controlled response is proportional to the PGA likewise the uncontrolled one. Therefore, in Fig. 3 and in Table 2 the performance indices J_1, J_2, \dots, J_6 of the ideal LQR system are constant with the PGA. On the contrary, the performance index J_7 linearly increases with the PGA because is the ratio between the peak control force and the maximum actuators' capacity ($u_{max} = 1000 \text{ kN}$). Finally, J_8 , is a quadratic function of the PGA because it represents the normalized peak control power which is given by a product between velocities and control forces.

In Fig. 3 and in Table 2 the ideal LQR system reaches the maximum actuators' capacity $u_{max} = 1000 \text{ kN}$ ($J_7 = 1$) for values of the PGA that are around 0.10 g in all cases. At larger values of the PGA the LQR system would require larger actuators to work properly. On the contrary, the SDRE-based controller limits the maximum required control forces and the system works properly for any value of the PGA.

The SDRE-based control system is essentially linear up to the value of the PGA which corresponds to the first force saturation and, in this linear range, provides similar performances to the ideal LQR system (small differences between the two are due to time delay and to the circumstance that $r_{i,i} \cong 0, i = 1, 2, \dots, m$, in Eq. (29)). The SDRE-based control system becomes non-linear after the actuators have reached their saturation limit. In this case, a progressive (non-linear) loss of control effectiveness takes place as the PGA is increased.

In the case of El Centro, the loss of control effectiveness caused by force saturation is seen to be relatively small, while in the cases of Northridge and Kobe is more significant. Also in these cases, however, the control performances are remarkable in reducing RMS response quantities despite force saturations. Clearly, the higher is the saturation limit the better are the control performances of the saturation control strategy in the non-linear range, as it is apparent looking at the results corresponding to 2500 kN and 5000 kN actuators in Fig. 3 and in Table 2.

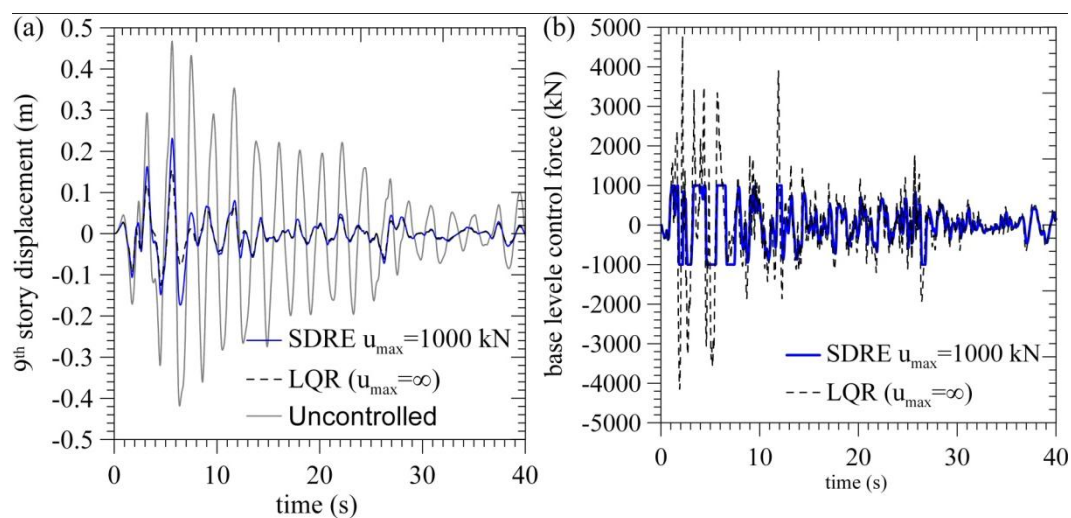


Fig. 4 Comparison between the response with ideal LQR control (dashed line) and with active saturation control (continuous line) under El Centro ground motion (PGA 0.50 g)

The reduction of the peak control power that is required by the SDRE-based saturation approach with respect to the ideal LQR system is also worth noting in Fig. 3 and in Table 2.

A sample response of the saturation system for a PGA of 0.50 *g*, compared with the uncontrolled and ideal LQR cases, is shown in Fig. 4 considering the seismic record of El Centro.

5.4 Semi-active control using MR dampers and comparison with active control

In the semi-active control strategy, nine MR dampers with the same characteristics of those adopted by Jung *et al.* (2003) are employed. The parameters of these MR dampers to be introduced in Eqs. (15) and (16) were experimentally determined in (Jung *et al.* 2003) and are also summarized in Table 3 for completeness sake. Considering their voltage limitation (10 V), the maximum capacity u_{\max} of such MR dampers is about equal to 1000 kN so being similar to that of the hydraulic actuators considered in the active system. The maximum instantaneous power of each semi-active device at 10 V is assumed to be equal to 50 Watt (Yoshida and Dyke 2004). For smaller values of the voltage this instantaneous power is simply scaled.

In the SDRE-based semi-active approach, parameter k_l , appearing in Eq. (21), was chosen as 10^3 as it was done in the active case. Also in this case k_l resulted from a calibration aimed at keeping the voltage saturation rate as small as possible not to produce undesired peaks of accelerations. Unitary state weight parameters Q_1, Q_2, \dots, Q_{2n} in Eq. (29) were adopted, while weights on control forces r_1, r_2, \dots, r_m were assumed equal to $2 \cdot 10^{-14}$. The quantities $r_{1,i}$ in Eq. (28) were chosen equal to 10^{-16} and online increased to 10^{-10} during the motion after the occurrence of the first force saturation.

The performances of the SDRE-based semi-active control strategy are compared with those of the SDRE-based active solution with similar maximum control force ($u_{\max} = 1000 \text{ kN}$). The results are presented in Fig. 5 and in Table 4 in the cases of the El Centro, Kobe and Northridge ground motions for a PGA varying up to 0.60 *g*.

First of all, it should be noticed that the semi-active control system is non-linear both for small and large values of the PGA. Indeed, the nonlinearity is, in this case, not only due to voltage saturation but also to the hysteretic behavior of the MR dampers. Therefore, a nonlinear variation of the performance indices with the PGA is observed in all the considered range of the PGA.

The results presented in Fig. 5 and in Table 4 show that the performances of the semi-active system are very close to those of the active one even if the MR dampers can only provide dissipative forces and require a control power that is extremely low.

It should be also mentioned that the differences between the performances of semi-active and active systems tend to be reduced as the PGA is increased. Indeed, the SDRE-based semi-active system exhibits slightly poorer control performances at very small values of the PGA because small structural responses do not activate significant hysteretic cycles in the MR dampers. On the contrary, the control performances of the semi-active system tend to improve, at first, as the PGA is increased, and, then, their worsening with the increase in the PGA due to voltage saturation appears to be much slower than in the active system. In some cases, the semi-active system performs even better than the active one because the peaks of control force can be higher than 1000 kN at a voltage of 10 V.

A sample semi-actively controlled response, compared with the ideal LQR controlled one, is shown in Fig. 6 considering the seismic record of El Centro with a PGA of 0.50 *g*.

Table 3 MR dampers parameters adopted in the analysis (Jung *et al.* 2003)

Semi-active control system characteristic	Value
α_a (kN/m)	26.0
α_b (kN·V/m)	29.1
c_{0a} (kN·s/m)	105.4
c_{0b} (kN·s·V/m)	131.6
γ (m ⁻²)	141.0
β (m ⁻²)	141.0
\bar{n}	2
η (s ⁻¹)	100

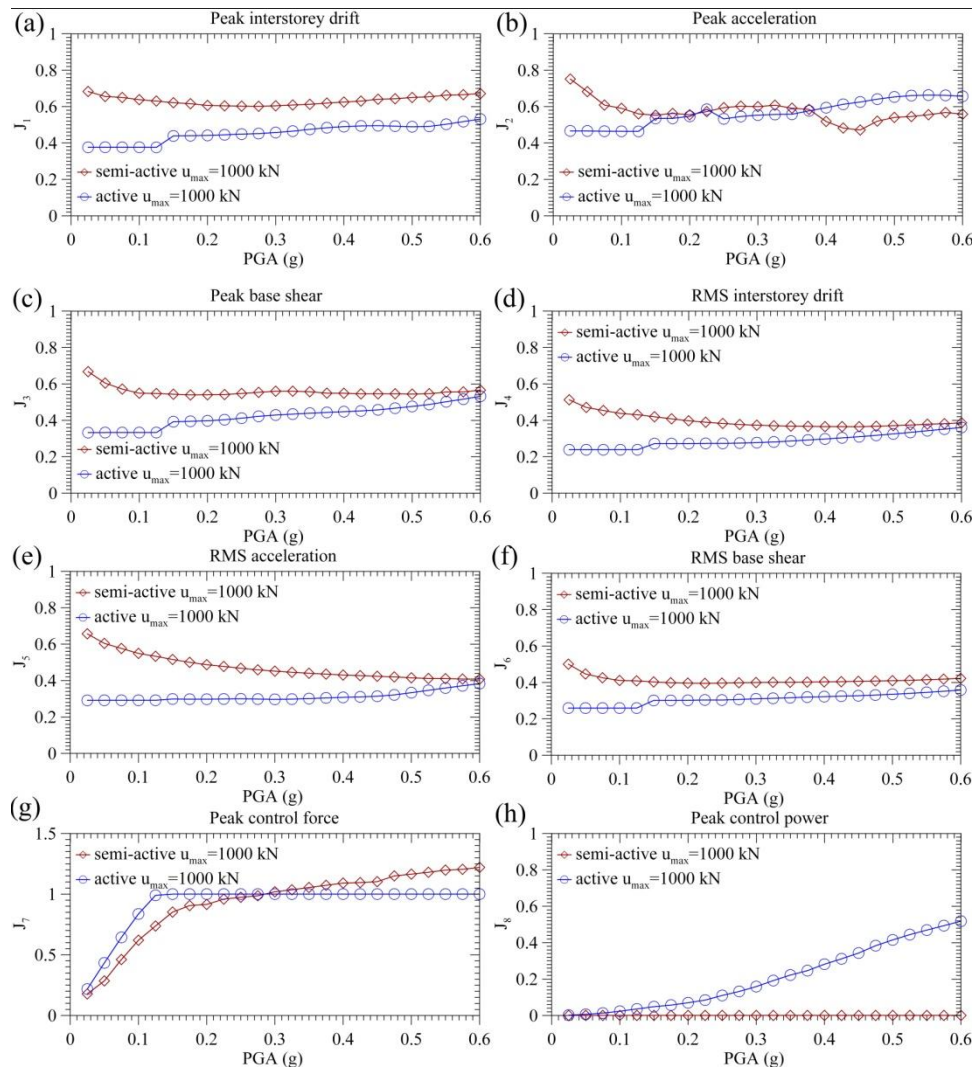


Fig. 5 Performances of semi-active and active saturation control systems with $u_{max}=1000$ kN under El Centro ground motion

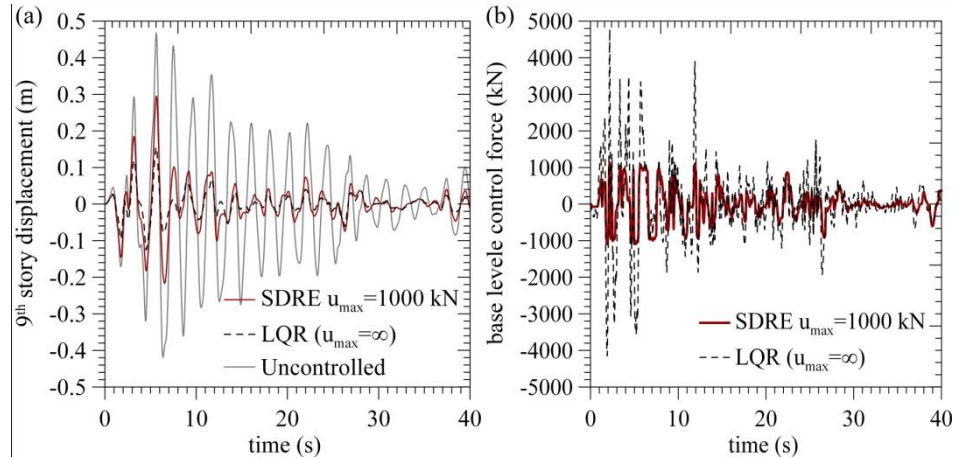


Fig. 6 Comparison between the response with ideal LQR control (dashed line) and with semi-active saturation control (continuous line) under El Centro ground motion (PGA 0.50 g)

Table 4 Performances of semi-active and active saturation control systems with $u_{\max}=1000$ kN under Kobe and Northridge ground motions

PGA (g)	Kobe						Northridge						
	0.1	0.2	0.3	0.4	0.5	0.6	0.1	0.2	0.3	0.4	0.5	0.6	
J ₁	Active	0.47	0.47	0.47	0.47	0.47	0.47	0.43	0.43	0.43	0.43	0.43	0.43
	Semi-Active	0.74	0.78	0.78	0.79	0.80	0.82	0.70	0.65	0.67	0.69	0.72	0.75
J ₂	Active	0.45	0.45	0.45	0.45	0.45	0.45	0.37	0.37	0.37	0.37	0.37	0.37
	Semi-Active	0.76	0.77	0.76	0.72	0.77	0.78	0.50	0.47	0.43	0.39	0.38	0.42
J ₃	Active	0.47	0.47	0.47	0.47	0.47	0.47	0.31	0.31	0.31	0.31	0.31	0.31
	Semi-Active	0.74	0.79	0.79	0.79	0.80	0.81	0.54	0.49	0.51	0.51	0.52	0.54
J ₄	Active	0.27	0.27	0.27	0.27	0.27	0.27	0.22	0.22	0.22	0.22	0.22	0.22
	Semi-Active	0.51	0.43	0.43	0.44	0.45	0.47	0.48	0.41	0.36	0.35	0.36	0.38
J ₅	Active	0.33	0.33	0.33	0.33	0.33	0.33	0.30	0.30	0.30	0.30	0.30	0.30
	Semi-Active	0.61	0.50	0.46	0.46	0.47	0.48	0.54	0.46	0.40	0.38	0.37	0.38
J ₆	Active	0.31	0.31	0.31	0.31	0.31	0.31	0.30	0.30	0.30	0.30	0.30	0.30
	Semi-Active	0.53	0.49	0.48	0.49	0.51	0.53	0.49	0.46	0.44	0.44	0.45	0.47
J ₇	Active	1.51	3.01	4.52	6.03	7.53	9.04	1.22	2.44	3.66	4.88	6.10	7.32
	Semi-Active	0.90	1.10	1.18	1.26	1.41	1.53	0.75	1.01	1.09	1.16	1.24	1.34
J ₈	Active	0.03	0.11	0.25	0.44	0.69	1.00	0.03	0.11	0.25	0.44	0.69	1.00
	Semi-Active	0.00	0.00	0.00	0.00	0.00	0.00	0.00	0.00	0.00	0.00	0.00	0.00

5.5 Comparison with existing saturation control techniques

A relatively standard approach to test the effectiveness of saturation controllers is to perform a comparison with an LQR approach calibrated to yield a maximum control force equal to the force saturation constraint. Lim *et al.* (2006) presented a similar analysis for a three story frame structure

equipped with one actuator, showing that saturation control techniques such as modified bang-bang control, saturated sliding mode control and the robust controller proposed by Lim *et al.* (2006) all provide similar performances and substantially improve the performance of calibrated LQR in reducing peak interstory drifts, while slightly improving such a performance in controlling peak accelerations. In particular, in the example presented by Lim *et al.* (2006) J_1 varied from 0.66 to about 0.38 while J_2 varied from 0.58 to about 0.54. Other performance indexes were not considered by the authors in that comparative study.

The proposed SDRE-based active saturation control with $u_{max}=1000$ kN is here compared to the LQR control calibrated to have the maximum value of the control force equal to 1000 kN at a PGA of 0.60g for the El Centro ground record. The calibration was performed using the same values of the state weights Q_1, Q_2, \dots, Q_{2n} adopted in the SDRE-based approach while calibrating r_1, r_2, \dots, r_m until the desired value of 1000 kN of the maximum control force was achieved. As a result, $\bar{r} = r_1 = r_2 = \dots r_m = 7.5 \cdot 10^{-13}$ was chosen.

Table 5 Performances of proposed active and LQR control strategy under El Centro ground motion

	PGA (g)	0.05	0.10	0.15	0.20	0.25	0.30	0.35	0.40	0.45	0.50	0.55	0.50
J_1	LQR	0.78	0.78	0.78	0.78	0.78	0.78	0.78	0.78	0.78	0.78	0.78	0.78
	<u>Proposed</u>	0.38	0.38	0.44	0.44	0.45	0.46	0.48	0.49	0.49	0.49	0.50	0.53
J_2	LQR	0.67	0.67	0.67	0.67	0.67	0.67	0.67	0.67	0.67	0.67	0.67	0.67
	<u>Proposed</u>	0.47	0.46	0.53	0.55	0.53	0.55	0.56	0.59	0.62	0.65	0.66	0.66
J_3	LQR	0.75	0.75	0.75	0.75	0.75	0.75	0.75	0.75	0.75	0.75	0.75	0.75
	<u>Proposed</u>	0.33	0.33	0.39	0.40	0.41	0.43	0.44	0.45	0.46	0.48	0.50	0.53
J_4	LQR	0.61	0.61	0.61	0.61	0.61	0.61	0.61	0.61	0.61	0.61	0.61	0.61
	<u>Proposed</u>	0.24	0.24	0.27	0.27	0.27	0.28	0.29	0.30	0.31	0.33	0.34	0.36
J_5	LQR	0.62	0.62	0.62	0.62	0.62	0.62	0.62	0.62	0.62	0.62	0.62	0.62
	<u>Proposed</u>	0.29	0.29	0.30	0.30	0.30	0.30	0.30	0.31	0.31	0.33	0.36	0.38
J_6	LQR	0.60	0.60	0.60	0.60	0.60	0.60	0.60	0.60	0.60	0.60	0.60	0.60
	<u>Proposed</u>	0.26	0.26	0.30	0.30	0.30	0.31	0.32	0.32	0.33	0.33	0.35	0.36
J_7	LQR	0.08	0.17	0.25	0.33	0.42	0.50	0.58	0.67	0.75	0.83	0.92	1.00
	<u>Proposed</u>	0.43	0.84	1.00	1.00	1.00	1.00	1.00	1.00	1.00	1.00	1.00	1.00
J_8	LQR	0.00	0.01	0.03	0.06	0.09	0.12	0.17	0.22	0.28	0.34	0.42	0.50
	<u>Proposed</u>	0.01	0.02	0.05	0.07	0.11	0.16	0.22	0.28	0.34	0.41	0.47	0.52

The results are presented in Table 5 and show that the proposed method allows to improve the performance of the LQR especially in reducing RMS interstory drifts and RMS accelerations. Fixing the attention to the results achieved considering a PGA of 0.6g, J_4 is reduced from 0.61 to 0.36 and J_5 from 0.62 to 0.38. The reduction of peak interstory drifts is also remarkable (J_1 from 0.78 to 0.53) and close to that achieved by other saturation techniques in (Lim *et al.* 2006), while the improvement in reducing peak accelerations is marginal which, however, is also the case when considering other techniques (Lim *et al.* 2006).

In the semi-active case the proposed SDRE-based approach can be regarded as a generalization of the modified clipped optimal control (MCO) where, as better commented in the following subsection, the generalization consists of the possibility of incorporating in the problem a broader

class of non-linearities and control constraints. Table 5 presents a comparison between the performances of the proposed semi-active control strategy and the MCOC considering the El Centro ground motion scaled at different values of the PGA. For a fair comparison between the two methods, full state knowledge and no time delay are assumed in this analysis. The performances of the proposed approach are sometimes slightly better and sometimes slightly worse than those yielded by MCOC. In general they are quite similar, hence allowing to conclude that the performances of the two methods are essentially equivalent when only force saturation is considered as control constraint.

Although it is not in the intentions of this work to present a systematic comparison of the proposed method with other existing saturation techniques, the presented results show that in presence of force saturation constraints the proposed approach provides control performances that are similar to those of other existing methods, both in active and semi-active cases. As discussed in next subsection, however, the proposed approach offers considerable advantages over existing techniques that could make it more attractive.

Table 6. Performances of proposed semi-active and modified clipped optimal control (MCOC) strategy under El Centro ground motion

	PGA (g)	0.05	0.10	0.15	0.20	0.25	0.30	0.35	0.40	0.45	0.50	0.55	0.50
J ₁	Proposed	0.59	0.46	0.44	0.45	0.48	0.52	0.52	0.54	0.56	0.58	0.61	0.63
	MCOC	0.51	0.46	0.44	0.46	0.48	0.51	0.54	0.56	0.58	0.60	0.62	0.64
J ₂	Proposed	1.11	1.14	1.00	0.84	0.73	0.63	0.57	0.52	0.48	0.49	0.49	0.49
	MCOC	1.15	1.13	1.03	0.82	0.72	0.60	0.52	0.50	0.49	0.50	0.49	0.48
J ₃	Proposed	0.47	0.40	0.38	0.41	0.43	0.44	0.44	0.46	0.47	0.49	0.51	0.53
	MCOC	0.46	0.37	0.37	0.42	0.44	0.45	0.46	0.48	0.49	0.50	0.52	0.54
J ₄	Proposed	0.38	0.30	0.27	0.27	0.27	0.28	0.28	0.30	0.31	0.32	0.34	0.35
	MCOC	0.35	0.29	0.27	0.27	0.27	0.28	0.29	0.30	0.31	0.33	0.34	0.35
J ₅	Proposed	0.64	0.53	0.48	0.43	0.40	0.38	0.37	0.35	0.35	0.35	0.35	0.36
	MCOC	0.58	0.47	0.41	0.37	0.36	0.35	0.34	0.34	0.34	0.34	0.34	0.35
J ₆	Proposed	0.38	0.33	0.31	0.31	0.31	0.32	0.32	0.34	0.35	0.36	0.37	0.39
	MCOC	0.38	0.32	0.30	0.30	0.31	0.32	0.33	0.34	0.35	0.36	0.37	0.39
J ₇	Proposed	0.44	0.81	0.93	0.96	1.00	1.03	1.07	1.09	1.13	1.16	1.19	1.22
	MCOC	0.39	0.82	0.92	0.96	0.99	1.03	1.06	1.09	1.13	1.16	1.19	1.22
J ₈	Proposed	0.00	0.00	0.00	0.00	0.00	0.00	0.00	0.00	0.00	0.00	0.00	0.00
	MCOC	0.00	0.00	0.00	0.00	0.00	0.00	0.00	0.00	0.00	0.00	0.00	0.00

5.6 Advantages of the proposed control strategy

The advantage of the proposed control technique when compared to existing saturation approaches, either active or semi-active ones, is twofold:

- it allows to include non-linearities in the formulation of the control problem;
- it allows to incorporate constraints on state variables, such as absolute displacements, interstory drifts, absolute velocities of actuators and more;

Another minor advantage of the proposed method compared to existing techniques is that it is relatively simple to be implemented because the procedure for solving the Riccati Equation is available in the library of most computational platforms.

Including non-linearities in the formulation of the control problem is possible by expressing the equation of motion in pseudo-linear form as in Eq. (1). This task requires to formulate a state-dependent system matrix $\mathbf{A}(\mathbf{x})$ which incorporates system non-linearities. Direct parametrization of the equations of motion is often not a practical way to calculate $\mathbf{A}(\mathbf{x})$ because most types of non-linearities that are encountered in practice are difficult to be expressed through non-linear state dependent terms. Nevertheless, an approximation of $\mathbf{A}(\mathbf{x})$ is generally achievable through online step-by-step numerical computations and such an approximation of $\mathbf{A}(\mathbf{x})$ is often sufficient because the SDRE is structurally stable. Among non-linearities that can be considered in this way are: geometric non-linearities, plasticization of frames, nonlinear constitutive behaviors of passive seismic devices, and more.

The most straightforward way to incorporate in the problem physical constraints on state variables, such as stroke limits of actuators, is to model such physical constraints using highly non-linear springs that produce negligible effects when the state variable is within the bounds, while producing large restoring forces when the physical limit is reached (see Friedland 1998). In order to avoid that such physical limits are attained during the motion, it is also convenient to introduce in Eq. (29) additional non-linear state dependent weights that strongly penalize the state variables when are approaching their physical limits. In this way it is possible, for instance, to achieve an effective control of maximum interstory drifts or maximum absolute displacements to prevent dangerous p-delta effects.

6. Conclusions

We have proposed an approach, based on the state dependent Riccati equation, for designing seismic response control strategies accounting for force saturation of control devices, system non-linearities and other control constraints. The method is an improvement of the one recently proposed by the authors for regulating an active mass damper with limited force and limited stroke. In particular, in this paper the method is applied to both active and semi-active control using MR dampers, also considering acceleration feedback, time delay compensation and state reconstruction. In the active case the proposed technique constitutes a generalization of the classic linear quadratic regulator while, in the semi-active case, it represents a novel generalization of the well-established modified clipped-optimal control strategy.

Although in this paper particular emphasis has been devoted to force saturation which is the main physical limitation that has to be considered in seismic control, the presented formulation is directly suitable to also consider constraints on structural displacements and to incorporate non-linearities, as well. This larger freedom with respect to existing techniques is achieved at the expense of an increase in computational complexity. Nevertheless, considering the ever growing computational speed of controllers available today in the market, it is believed that this aspect does not represent a significant drawback of the method.

The proposed approach has been mathematically illustrated with reference to a general multi-story frame structure equipped with an active bracing system or with its semi-active counterpart using magnetorheological dampers. Numerical simulations have been presented considering the ASCE benchmark 9-stories steel building subjected to different earthquake records scaled at increasing values of the PGA. The results have shown that the proposed methodology allows to achieve control performances that are remarkable in both active and semi-active cases,

even with significant force saturations at large values of the PGA. Such control performances are seen to be essentially equivalent to those provided by existing saturation control strategies. It is concluded therefore that the proposed technique is potentially more attractive than any other existing method because, along with a similar effectiveness, it also permits to account for various types of non-linearities and physical constraints.

Acknowledgements

This research was supported by a grant from the “Cassa di Risparmio di Perugia” Foundation (project number 2010.011.0490).

References

- Basu, B. and Nagarajaiah, S., (2008), “A wavelet-based time-varying adaptive LQR algorithm for structural control”, *Eng. Struct.*, **30**, 2470-2477.
- Beeler, S.C. (2004), *State-dependent Riccati equation regulation of systems with state and control nonlinearities*, NASA Technical Report.
- Breccolotti, M., Gusella, V. and Materazzi, A.L. (2007), “Active displacement control of a wind-exposed mast”, *Struct. Health Monit.*, **14**(4), 556-575.
- Cao, Y.Y., Lin, Z. and Ward, D.G. (2004), “Anti-windup design of output tracking systems subject to actuator saturation and constant disturbances”, *Automatica*, **40**, 1221-1228.
- Casciati, F., Magonette, G. and Marazzi, F. (2006), *Technology of semiactive devices and applications in vibrations mitigation*, Wiley, New York.
- Casciati, S. and Faravelli, L. (2008), “Structural components in shape memory alloy for localized energy dissipation”, *Comput. Struct.*, **86**, 330-339.
- Casciati, S. and Marzi, A. (2010), “Experimental studies on the fatigue life of shape memory alloy bars”, *Smart. Struct. Syst.*, **6**(1), 73-85.
- Cloutier, J.R. (1997), “State dependent Riccati equation techniques: an overview”, *Proceedings of the American Control Conference*, Albuquerque, NM, 4-6 June.
- Dyke, S.J., Spencer, B.F., Sain, M.K. and Carlson, J.D. (1996), “Modeling and control of magnetorheological dampers for seismic response reduction”, *Smart Mater. Struct.*, **5**, 565-575
- Erdem, E.B. (2001), *Analysis and real-time implementation of state-dependent Riccati equation controlled systems*, Ph.D. Dissertation, University of Illinois at Urbana-Champaign.
- Faravelli, L., Fuggini, F. and Ubertini, F. (2010), “Toward a hybrid control solution for cable dynamics: theoretical prediction and experimental validation”, *Struct. Health Monit.*, **17**(4), 386-403.
- Forrai, A., Hashimoto, S., Funato, H. and Kamiyama, K. (2003), “Robust active vibration suppression control with constraint on the control signal: application to flexible structures”, *Earthq. Eng. Struct. D.*, **32**, 1655-1676.
- Friedland, B. (1998), “On controlling systems with state-variable constraints”, *Proceedings of the American Control Conference*, Philadelphia, PA, U.S.A., 24-26 June.
- Gusella, V. and Materazzi, A.L. (1998), Non-Gaussian response of MDOF wind-exposed structures: analysis by bicoherence function and bispectrum, *Meccanica*, **33**(3), 299-307.
- Hong, A.L., Ubertini, F. and Betti, R. (2011), “Wind analysis of a suspension bridge: identification and finite-element model simulation”, *J. Struct. Eng.-ASCE*, **137**(1), 133-142.
- Indrawan, B., Kobori, T., Sakamoto, M., Koshika, N. and Ohri, S., (1996), “Experimental verification of bounded-force control method”, *Earthq. Eng. Struct. D.*, **25**(2), 79-193.
- Jung, H.J., Spencer Jr., B.F. and Lee, I.W. (2003), “Control of seismically excited cable-stayed bridge

- employing magnetorheological fluid dampers”, *J. Struct. Eng.-ASCE*, **129**(7), 873-883.
- Kobori, T., Takahashi, M., Nasu, T., Niwa, N. and Ogasawara, K. (1993), “Seismic response controlled structure with active variable stiffness system”, *Earthq. Eng. Struct. D.*, **22**(11), 925-941.
- Lim, C.W., Park, Y.J. and Moon, S.J., (2006), “Robust saturation controller for linear time-invariant system with structured real parameter uncertainties”, *J. Sound Vib.*, **294**(1-2), 1-14.
- Lim, C.W. (2007), “Remarks on robust stability of saturation controllers”, *J. Sound Vib.*, **299**(1-2), 363-372.
- Lim, C.W. (2008), “Active vibration control of the linear structure with an active mass damper applying robust saturation controller”, *Mechatronics*, **18**, 391-399.
- Materazzi, A.L. and Ubertini, F. (2012), “Robust structural control with system constraints”, *Struct. Health Monit.*, **19**, 472-490.
- Mongkol, J., Bhartia, B.K. and Fujino, Y. (1996), “On linear saturation (LS) control of buildings”, *Earthq. Eng. Struct. D.*, **25**, 1353-1371.
- Mracek, C.P. and Cloutier, J.R. (1998), “Control designs for the nonlinear benchmark problem via the state-dependent riccati equation method”, *Int. J. Robust Nonlin.*, 401-433.
- Nagarajaiah, S. and Narasimhan, S. (2007), “Seismic control of smart base isolated buildings with new semiactive variable damper”, *Earthq. Eng. Struct. D.*, **36**, 729-749.
- Narasimhan, S. (2009), “Robust direct adaptive controller for the nonlinear highway bridge benchmark”, *Struct. Health Monit.*, **16**(6), 599-612
- Ohtori, Y., Christenson, R.E., Spencer Jr., B.F. and Dyke, S.J. (2004), “Benchmark control problems for seismically excited nonlinear buildings”, *J. Eng. Mech-ASCE*, **130**(4), 366-385.
- Panariello, G.F., Betti, R. and Longman, R.W. (1997). “Optimal structural control via training on ensemble of earthquakes”, *J. Eng. Mech-ASCE*, **123**(11), 1170-1179.
- Reinhorn, A.M., Soong, T.T., Riley, M.A., Lin, R.C., Aizawa, S. and Higashino, M. (1993), “Full-scale implementation of active control. II: installation and performance”, *J. Struct. Eng.-ASCE*, **119**(6), 1935-1960.
- Renzi, E. and Serino, G. (2004), “Testing and modelling a semi-actively controlled steel frame structure equipped with MR dampers”, *Struct. Health Monit.*, **11**, 189-221.
- Soong, T.T. (1990), *Active structural control: theory and practice*, Longman Scientific & Technical, Essex, England.
- Suresh, S., Narasimhan, S., Nagarajaiah, S. and Sundararajan, N. (2010), “Fault-tolerant adaptive control of nonlinear base-isolated buildings using EMRAN”, *Eng. Struct.*, **32**, 2477-2487.
- Symans, M.D., Charney, F.A., Whittaker, A.S., Constantinou, M.C., Kircher, C.A., Johnson, M.W. and McNamara, R.J. (2008), “Energy dissipation systems for seismic applications: current practice and recent developments”, *J. Struct. Eng.-ASCE*, **134**(1), 3-21.
- Ubertini, F. (2008), “Active feedback control for cable vibrations”, *Smart Struct. Syst.*, **4**(4), 407-428.
- Ubertini, F. (2010), “Prevention of suspension bridge flutter using multiple tuned mass dampers”, *Wind Struct.*, **13**(3), 235-256.
- Varadarajan, N. and Nagarajaiah, S. (2004), “Wind response control of building with variable stiffness tuned mass damper using EMD/HT”, *J. Eng. Mech-ASCE*, **130**(4), 451-458.
- Wu, Z. and Soong, T.T. (1996). “Modified bang-bang control law for structural control implementation”, *J. Eng. Mech.-ASCE*, **122**(8), 771-777.
- Yan, N., Wang, C.M. and Balendra, T. (1999), “Optimal damper characteristics of ATMD for buildings under wind loads”, *J. Struct. Eng.-ASCE*, **125**(12), 1376-1383.
- Yang, G., Spencer Jr., B.F., Carlson, J.D. and Sain, M.K. (2002), “Large-scale MR fluid dampers: modeling and dynamic performance considerations”, *Eng. Struct.*, **24**, 309-323.
- Ying, Z.G., Ni, Y.Q. and Ko, J.M. (2007), “A bounded stochastic optimal semi-active control”, *J. Sound Vib.*, **304**(3-5), 948-956.
- Yoshida, O. and Dyke, S.J. (2004), “Seismic control of a nonlinear benchmark building using smart dampers”, *J. Eng. Mech-ASCE*, **130**(4), 386-392.